SLAC-PUB 5951
UND-HEP-92-BIG05
DTP-92-62
September 1992
(T/E)

PHOTON LINEAR COLLIDERS AS ALADDIN'S LAMP – NOVEL PROBES OF QCD IN $t\bar{t}$ PHYSICS*

I. I. Bigi and **F. Gabbiani**

Dept. of Physics, University of Notre Dame du Lac, Notre Dame, IN 46556, USA
bitnet: "BIGI@UNDHEP", "GABBIANI@UNDHEP"
decnet: UNDHEP::BIGI, UNDHEP::GABBIANI

V. A. Khoze

Stanford Linear Accelerator Center, Stanford University, Stanford, CA 94309, USA
and
Department of Physics, University of Durham, Durham DH1 3LE, England
bitnet: "KHOZE@SLACVM","KHOZE@CERNVM"

Abstract

S-wave and P-wave production cross sections of top quarks in the threshold region are obtained from perturbative QCD in terms of m_t, Γ_t and α_S. S-wave production is described in terms of the Green's function for the $t\bar{t}$ system whereas P-wave production depends on the second space derivatives of the $t\bar{t}$ Green's function. We show by explicit calculation that those relativistic corrections that a priori could affect specifically the non-S-wave production are quite insignificant if top decays mainly like $t \to bW$ or $t \to bH$ with H denoting a charged Higgs state. A comparison of the S-wave and P-wave case thus provides a novel probe of QCD as it affects top dynamics. Collisions of polarized photons off each other allow to extract separately the S-wave and P-wave production cross section. Such polarized photon beams can be generated by Compton backscattering laser light off polarized electron and positron beams.

Submitted to *Nuclear Physics B*

* This work was supported in part by National Science Foundation Grant PHY-89-09929,
by Department of Energy contract DE–AC03–76SF00515,
and by the United Kingdom Science and Engineering Research Council.

1. Introduction

Top quarks have not been discovered yet and a non-trivial lower bound on their mass has been established:

$$m_t \geq 91 \text{ GeV} \tag{1.1}$$

Yet due to various indirect lines of reasoning there exists little doubt that

– top quarks as defined in the Standard Model do exist in nature

– with a mass that is probably in the range of 100 – 200 GeV or there about.

This range suggests that top quarks should be discovered in the foreseeable future and that accelerators are feasible that would allow a detailed study of top production and decay.

It has been realized more and more in recent years that the physics of very heavy top quarks has many redeeming features [1]. One particularly intriguing observation is that the top decay width provides an infrared cut-off for the strong forces between top quarks and antiquarks [2]. The semi-weak width for the decay $t \to b + W$ actually rises so quickly with the top mass that for $m_t \geq 130 - 140$ GeV *perturbative* QCD suffices to treat the threshold production of top quarks. One can actually deal with S-wave and P-wave production separately: the former can be expressed in terms of the Schrödinger Green's function describing the relative motion of the top quark and antiquark produced; the latter involves two space derivatives of this Green's function. There arises a further distinction between the two cases [3]: while one can show that S-wave production can be described in a non-relativistic picture sufficiently close to threshold, this is not necessarily true any longer in P [D etc.]-wave production. For in general there arise high-momentum contributions which are controlled by the off-shell behaviour of the top decay width. Yet for a given top decay process one can determine $\Gamma_t(p^2)$ and thus compute such relativistic corrections. We will show below that for the decays $t \to b + W^+$ or $t \to b + H^+$ these corrections are numerically irrelevant. A non-relativistic description is thus a posteriori justified both for S- and P-wave production of top quarks right at threshold.

The threshold production cross section is calculated in terms of m_t, Γ_t and α_S. Since, as already stated, S-wave [P-wave] production depends on the Green's function [second space derivative of the Green's function] for the $t\bar{t}$ system a study of top threshold production that disentangles contributions from S- and P-wave configurations thus provides us with novel and independent probes of top dynamics. More specifically it would allow an experimental extraction of the three parameters m_t, Γ_t and even α_S with high accuracy and in a way that is systematically different from other methods.

Alas, this is easier said than done! The reaction $e^+e^- \to t\bar{t}$ yields predominantly an S-wave configuration; it appears unlikely that the small admixture of P-wave production could be extracted; hadronic production holds out even less promise of separating S- and P-wave production; this is compounded by the fact that the $t\bar{t}$ pairs are there produced both in a colour singlet and octet configuration [4].

A Photon Linear Collider (hereafter referred to as PLC) provides new opportunities here. A PLC is a facility where high energy photon beams are generated by Compton backscattering of laser photons off high energy electron beams; those photon beams are then brought into collision with another similarly obtained photon beam. Such beams possess a threefold advantage for our analysis [5]:

(1) High luminosity photon beams can be achieved in such an environment. One might actually achieve higher luminosities here than in direct e^+e^- annihilation!

(2) There are neither appreciable beam-beam effects nor initial beam radiation that could affect adversely the measurements.

(3) Using polarized electron beams and lasers one might be able to prepare quite *monochromatic* photon beams with a high degree of polarization [5,6]. Changing the polarization of the photon beams will allow us to separate S-wave and P-wave production of top quarks.

Our paper will be organized as follows: in sect. 2 we list the expressions for the decays $t \to b + W$, $b + H$; in sect. 3 we recapitulate S-wave top production whereas in sect. 4 we describe P-wave production; there we also demonstrate that relativistic corrections can be ignored; in sect. 5 we present the formulae for the collisions of polarized photons and show how S- and P-wave production can be distinguished; our summary is finally presented in sect. 6.

2. Top Decay Width

In general one cannot treat the production of heavy quarks near threshold perturbatively since there one encounters infrared singularities reflecting resonance formation etc. Yet the decay width of the produced quarks provides an infrared cut-off that removes these singularities or at least softens them; if the decay width is sufficiently large, the threshold production can be treated with perturbative QCD without recourse to a phenomenological model.

Our discussion of how large a decay width is expected for top quarks does not contain any new findings at this point; we present it here for completeness and also because it will lead to a new result in the subsequent analysis.

According to the lower bound stated in eq. (1.1) top quarks are sufficiently heavy to undergo the semiweak decay $t \to W^+ + b$ [1]:

$$\Gamma(t \to W^+ + b) = \frac{G_F m_t^3}{8\pi\sqrt{2}} \left(\frac{2P_W}{m_t}\right) \left[\left(1 - \frac{m_b^2}{m_t^2}\right)^2 + \frac{m_W^2}{m_t^2}\left(1 + \frac{m_b^2}{m_t^2}\right) - \frac{2m_W^4}{m_t^4} \right], \tag{2.1}$$

where

$$P_W = \left\{[m_t^2 - (m_W + m_b)^2][m_t^2 - (m_W - m_b)^2]\right\}^{1/2} / (2m_t). \tag{2.2}$$

Extensions of the Standard Model like SUSY contain charged Higgs fields; those could also be lighter than top quarks thus allowing the transition $t \to H^+ + b$ which adds to the decay width:

$$\Gamma(t \to H^+ + b) = \frac{G_F m_t^3}{8\pi\sqrt{2}} \left(1 + \frac{m_b^4}{m_t^4} + \frac{m_H^4}{m_t^4} - 2\frac{m_b^2}{m_t^2} - 2\frac{m_H^2}{m_t^2} - 2\frac{m_b^2 m_H^2}{m_t^4}\right)^{1/2} \times \left[\left(\cot^2\beta + \frac{m_b^2}{m_t^2}\tan^2\beta\right)\left(1 + \frac{m_b^2}{m_t^2} - \frac{m_H^2}{m_t^2}\right) + 4\frac{m_b^2}{m_t^2}\right], \tag{2.3}$$

The SM mode, eq. (2.1), yields a width of 100 MeV for m_t = 100 GeV and 1 GeV for m_t = 160 GeV. The weight of the Higgs mode, eq. (2.3), depends on the size of the V.E.V.'s v_1, v_2; if they satisfy the relation

$$1 \lesssim \tan\beta = \frac{v_2}{v_1} \lesssim \frac{m_t}{m_b} \sim 30 \tag{2.4}$$

(as obtained in Grand Unification schemes) then the width for the Higgs mode is somewhat smaller than for the W mode; otherwise it could be larger. For completeness we will include this decay mode in our subsequent analysis. In any case for $m_t \geq 120$ GeV a *perturbative* treatment of top *threshold* production becomes more and more reliable numerically.

3. S-Wave Top Production

Gluon exchanges between the produced top quark and antiquark generate contributions that depend on α_S/β_t rather than just α_S; this is in close analogy to the case of Coulomb exchanges in QED [7]. These terms are dominant close to threshold where $\beta_t \ll 1$ holds; they change the S-wave Born cross section which vanishes at threshold proportional to β_t into an expression proportional to α_S, i.e. finite right at threshold. Once these leading contributions are summed to all orders in α_S/β_t, toponium resonance formation is reproduced. This can actually be described by a multiplicative correction of the Born cross section that depends on the orbital angular momentum, the colour quantum number and the energy of the produced $t\bar{t}$ pair [2,3]. In gamma gamma production of top one deals with colour singlet configurations; one then finds:

$$d\sigma_S(\gamma\gamma \to t\bar{t}) = d\sigma_S^{(B)}(\gamma\gamma \to t\bar{t})\frac{K_S^{(1)}(E)}{K_S^{(B)}(E)}. \tag{3.1}$$

$d\sigma_S^{(B)}$ denotes the Born result for the differential cross section; the correction factor is expressed as the ratio of two functions of E, the amount of energy that exceeds the threshold

$$E = W - 2m_t. \tag{3.2}$$

These functions are given by [2]

$$K_S^{(1)}(E) = \mathrm{Im}G^{(1)}(0, 0, E + i\Gamma_t), \tag{3.3}$$

where $G^{(1)}$ is the $l = 0$ component of the Schrödinger Green's function for the relative motion of the top quarks in a colour singlet state:

$$G^{(1)}(\vec{r}, \vec{r}\,', E + i\Gamma_t) = \langle \vec{r}\, | [H^{(1)} - (E + i\Gamma_t)]^{-1} | \vec{r}\,' \rangle. \tag{3.4}$$

The non-relativistic Hamilton operator $H^{(1)}$ contains the potential for colour singlet $t\bar{t}$ configurations. The quantity $K_S^{(B)}$ finally is the Born approximation to K_S:

$$K_S^{(B)}(E) = \frac{m_t}{4\pi}(m_t E)^{1/2}. \tag{3.5}$$

Assuming a fixed strong coupling α_S one can give an analytical expression for $K_S^{(1)}(E)$:

$$\begin{aligned} K_S^{(1)}(E) = \mathrm{Im} G^{(1)}(0, 0, E + i\Gamma_t) = \frac{m_t^2}{4\pi} \Bigg\{ & \frac{k_+}{m_t} + \frac{2k_1}{m_t} \arctan \frac{k_+}{k_-} \\ & + \sum_{n=1}^{\infty} \frac{2k_1^2}{m_t^2 n^4} \frac{\Gamma_t k_1 n + k_+[n^2\sqrt{E^2 + \Gamma_t^2} + k_1^2/m_t]}{[E + k_1^2/(m_t n^2)]^2 + \Gamma_t^2} \Bigg\}, \end{aligned} \tag{3.6}$$

with

$$k_1 = \frac{2}{3}\alpha_S m_t, \tag{3.7}$$

$$k_\pm = \sqrt{\frac{m_t}{2}\left(\sqrt{E^2 + \Gamma_t^2} \pm E\right)}. \tag{3.8}$$

The expression in (3.6) can be interpreted in a straightforward fashion: the first two terms in the curly bracket describe *continuum* production of top quarks while the third sums over the toponium *resonances.*

To include the effects caused by the "running" of α_S one can evaluate the Green's function numerically as done in ref. [8]. Using their algorithm we have calculated the cross-section ratio $R_{tt} = \sigma_S(\gamma\gamma \to t\bar{t})/\sigma(e^+e^- \to \mu^+\mu^-)$ and plotted it against E in GeV for in the S-wave case for m_t = 100, 130, 150 and 200 GeV, where

$$\sigma(e^+e^- \to \mu^+\mu^-) = \frac{4\pi\alpha^2}{3W^2}. \tag{3.9}$$

In addition to the colour Coulomb exchanges we have also included the hard gluon exchange corrections and gluon bremsstrahlung off the final state quarks [8,9] which are of order α_S rather than α_S/β_t. For the cross-section this gives [10] a factor

$$1 - \frac{4}{3}\frac{\alpha_S(4m_t^2)}{\pi}\left(5 - \frac{\pi^2}{4}\right). \tag{3.10}$$

For photon beams the heights of the resonance curves are not reduced or modified by initial state radiation as it was the case in the analysis of refs. [3,8,11]. For $\alpha_S(m_Z)$ = 0.12 our results are given in fig. 1 [fig. 2] with the top decays assumed to proceed like

$t \to bW$ [$t \to bW$, $t \to bH$]; the dashed curves represent the Born result. We want to draw attention to the following observations:

- A clear resonance structure emerges for "light" top quarks with $m_t = 100$ GeV. It quickly fades away with increasing m_t and has disappeared for $m_t = 200$ GeV.
- Very sizeable threshold enhancements in the cross section occur even apart from the obvious resonance peaks.
- The detailed shape of the excitation curve depends on the decay width of the top quarks. For fig. 2 it was assumed that the top decay width is enhanced by 50% over the Standard Model expectations as it could happen if the decay channel $t \to b + H$ were available. While the position of the resonance peaks and the open top plateau remain unaffected – as expected – the height of the peaks do change, in particular for "light" top quarks. If on the other hand the top decay width is smaller than expected – say because the KM parameter $|V(tb)|$ is (in contrast to a three family ansatz) appreciably below unity – then the resonance peaks will be enhanced, while their positions remain unaffected.
- To reveal these intriguing structures one needs the energy of the photon beams defined to better than a GeV.

4. P-Wave Top Production

An extension of this treatment to a P-wave $t\bar{t}$ production can be performed according to refs. [3]:

$$d\sigma_P(\gamma\gamma \to t\bar{t}) = d\sigma_P^{(B)}(\gamma\gamma \to t\bar{t}) \frac{K_P^{(1)}(E)}{K_P^{(B)}(E)}, \tag{4.1}$$

where the function $K_P^{(1)}$ which represents the impact of the strong final state interactions is given by

$$K_P^{(1)}(E) = \mathrm{Im} \left\langle \frac{\partial}{\partial \vec{r}} \frac{\partial}{\partial \vec{r}\,'} G_E^{(1)}(\vec{r}, \vec{r}\,') \right\rangle_{\vec{r}=\vec{r}\,'=0}, \tag{4.2}$$

with $G_E^{(1)}(\vec{r}, \vec{r}\,')$ defined as in (3.4), but taking the $l = 1$ component of the Green's function in the singlet state. $K_P^{(B)}(E)$ finally denotes the Born expression:

$$K_P^{(B)}(E) = \frac{m_t}{4\pi}(m_t E)^{3/2}. \tag{4.3}$$

These final state interactions change the production cross section, which on the Born level is proportional to β^3, into an expression proportional to α_S^3, which is finite (although rather small) right at threshold.

There arises a new feature for non-vanishing orbital angular momenta: strictly speaking a nonrelativistic description a priori does not hold anymore since the loop integrals describing the invariant mass distribution of the decay products can now receive contributions from high top momenta. This new contribution does practically not depend on E and is given by

$$\widetilde{K}_P^{(1)} = 2m_t^2 \int_{\mu^2}^{m_t^2} \frac{(9m_t^2 - p^2)^{3/2}}{(2\pi)^2} \frac{\Gamma_t(p^2) dp^2}{(4m_t)^3 (m_t^2 - p^2)^{1/2}}, \tag{4.4}$$

where μ is the minimal invariant mass of the decay products, *i.e.* $m_{W^+} + m_b$ or $m_{H^+} + m_b$. $\Gamma_t(p^2)$ is the off-shell decay width for the top quark; in the unitary gauge it is obtained by replacing m_t^2 by p^2 in the on-shell decay formula (2.2):

$$\Gamma(p^2; t \to W^+ + b) = \frac{G_F p^3}{8\pi\sqrt{2}} \left(\frac{2P_W(p)}{p}\right) \left[\left(1 - \frac{m_b^2}{p^2}\right)^2 + \frac{m_W^2}{p^2}\left(1 + \frac{m_b^2}{p^2}\right) - \frac{2m_W^4}{p^4}\right], \quad (4.5)$$

with

$$P_W(p) = \left\{[p^2 - (m_W + m_b)^2][p^2 - (m_W - m_b)^2]\right\}^{1/2} / (2p). \quad (4.6)$$

It is rather straightforward to obtain the analogous expression for the decay $t \to H^+ + b$. For the case at hand (t decay into W and/or H^+), the integral (4.4) has proven to be numerically rather small and the validity of the nonrelativistic approximation has thus been established *a posteriori*; however its contribution has been added to $K_P^{(1)}(E)$.

The function $K_P^{(1)}(E)$ can be evaluated analytically for a fixed value of α_S:

$$\begin{aligned} K_P^{(1)}(E) = (k_1^2 + m_t E) K_S^{(1)}(E) + \frac{m_t^2 \Gamma_t}{4\pi} \Bigg\{ -k_- + 2k_1 \log\left|\frac{k_1}{k_- + ik_+}\right| \\ - \frac{2k_1^2}{m_t} \sum_{n=1}^{\infty} \frac{1}{n^3} \frac{(nk_- + k_1)(E + k_1^2/m_t n^2) - k_+ \Gamma_t}{[E + k_1^2/(m_t n^2)]^2 + \Gamma_t^2} \Bigg\}. \end{aligned} \quad (4.7)$$

To analyze the precise impact that the "running" of α_S has on the production cross section one has to compute $K_P^{(1)}$ numerically. Unfortunately the algorithm developed in ref. [8] for the S-wave case cannot be applied here since the effective potential is more singular for $l = 1$. To exploit the QCD analysis presented here to its fullest potential one needs a numerical procedure developed that allows to treat P-wave production. Lacking that for the moment we use a semi-quantitative ansatz similar to ref. [2] to gauge the impact of the "running" of α_S:

i) for each m_t we determined the value of E corresponding to the first resonance in the S-wave case;

ii) then we substituted $m_t\sqrt{E^2 + \Gamma_t^2}$ for r^{-2} in the two-loop expression for running α_S [8].

One gets $\alpha_S = 0.213$, $\alpha_S = 0.201$ and $\alpha_S = 0.195$ for $m_t = 100$, 130 and 150 GeV, respectively, for both $\Gamma_t = \Gamma(t \to W^+ + b)$ and $\Gamma_t = \Gamma(t \to W^+ + b) + \Gamma(t \to H^+ + b)$. For $m_t = 200$ GeV we get $\alpha_S = 0.179$ in the former case and $\alpha_S = 0.177$ in the latter.

Results for the cross-section ratio $R_{tt} = \sigma_P(\gamma\gamma \to t\bar{t})/\sigma(e^+e^- \to \mu^+\mu^-)$ are plotted as function of E [in GeV], the energy above threshold, for $m_t = 100$, 130, 150 and 200 GeV in fig. 3. The contributions of hard gluon exchanges and gluon bremsstrahlung to the cross sections are included through a correction factor [12]

$$1 - \frac{16}{3}\frac{\alpha_S(4m_t^2)}{\pi}. \quad (4.8)$$

The dashed lines again represent the Born result. The following observations should be noted:

• The P-wave production cross section right at threshold is rather small compared to the S-wave case. That is not surprising on quite general grounds: for the P-wave production cross section opens up very gradually at threshold, namely like β_t^3 for the Born contribution or like α_S^3 after summing over the colour Coulomb exchanges between the $t\bar{t}$ pair viz. β or α_S for S-wave production. The threshold enhancement due to the strong final state interactions is relatively much larger in the P-wave than in the S-wave case, yet it still yields a much smaller P-wave than S-wave cross section.

• A single resonance peak appears and even that only for the light top quark case of $m_t = 100$ GeV. This as well is easily understood qualitatively: due to the slow opening of P-wave production close to threshold – as mentioned above – only the spectacular resonance peaks can then surface. This also implies that perturbative QCD will yield a satisfactory description of P-wave production for lower values of the top mass than for S-wave production.

• The height and width of the resonance peak – if it is there – is sensitive to the size of Γ_t, i.e. whether $|V(tb)|$ is indeed very close to unity and/or whether there are other significant channels available for top decays.

5. Top Production in the Collisions of Polarized Photons

In the preceding sections we have treated the S-wave and P-wave case *separately* and for a *fixed c.m. energy.* We will describe now how the use of polarized photon beams will indeed allow to distinguish S-wave and P-wave production; we will also address the issue of the monochromaticity of the photon beams.

The Born cross section for the production of top quarks in the collisions of polarized photons is given by [13]

$$\begin{aligned}\sigma(\gamma\gamma \to t\bar{t}) = \frac{\pi\alpha^2 R}{W^2}\Bigg\{&2(3-\beta^4)\log\frac{1+\beta}{1-\beta} - 4\beta(2-\beta^2) + 4\xi_2^{(1)}\xi_2^{(2)}\left(3\beta - \log\frac{1+\beta}{1-\beta}\right)\\ &- \left(2\beta + \frac{1}{\gamma^2}\frac{1+\beta}{1-\beta}\right)\left[\frac{1}{\gamma^2}\left(\xi_3^{(1)}\xi_3^{(2)} - \xi_1^{(1)}\xi_1^{(2)}\right) + 2\beta\zeta_t\left(\xi_2^{(1)} + \xi_2^{(2)}\right)\right]\Bigg\},\end{aligned} \tag{5.1}$$

with

$$\gamma = \frac{W}{2m_t}, \qquad \beta = \sqrt{1 - 4m_t^2/W^2}, \qquad R = N_C e_t^4. \tag{5.2}$$

W is the c.m. energy of the reaction and e_t [N_C] the charge [colour factor] for the outcoming particles ($e_t = 2/3$ and $N_C = 3$ for top quarks); ζ_t denotes the helicity of the top quarks whereas the photon helicities are expressed by the Stokes parameters ξ's defined in ref. [14]: $\xi_2^{(1)}$ and $\xi_2^{(2)}$ denote the degree of circular polarization whereas $\xi_1^{(1,2)}$ and $\xi_3^{(1,2)}$ represent the amount of linear polarization of the two colliding photons. We will focus here on circularly polarized photon beams since laser backscattering appears to be able to produce them; therefore we will set $\xi_1^{(1,2)} = \xi_3^{(1,2)} = 0$ throughout this paper.

We are actually treating top production near threshold where $\beta \ll 1$ holds; summing over the quark helicities we obtain

$$\sigma_{\rm nonrel} = \frac{4\pi\alpha^2 R}{W^2}\left[\left(1+\xi_2^{(1)}\xi_2^{(2)}\right)\left(\beta+\frac{2}{3}\beta^3\right)+\left(1-\xi_2^{(1)}\xi_2^{(2)}\right)\frac{4}{3}\beta^3\right]. \tag{5.3}$$

If the two photons carry the *opposite* helicities, i.e. for $\xi_2^{(1)}\cdot\xi_2^{(2)} = -1$, the $t\bar{t}$ pair is produced in a pure *P-wave* state with $\sigma_P(t\bar{t}) \propto \beta^3$. It is easily understood why S-wave production vanishes for such a configuration: for the initial state then carries two units of angular momentum which cannot be made up by the two spin 1/2 quarks in an S-wave. If on the other hand the two photons carry the *same* helicities, *i.e.*for $\xi_2^{(1)}\cdot\xi_2^{(2)} = +1$, the $t\bar{t}$ pair is produced in an *S-wave* state with $\sigma_S(t\bar{t}) \propto \beta$.

It is worth mentioning here that the quark helicity ζ_t enters the expression for the cross section only in the combination $\zeta_t\left(\xi_2^{(1)}+\xi_2^{(2)}\right)$. This is due to parity invariance and Bose statistics for the photons.

The photons that can be produced from polarized electron and positron beams via the backscattering of laser light are circularly polarized. The corresponding differential Born cross section is given by [5,13]

$$\frac{d\sigma(\gamma_{cp}\gamma_{cp}\to t\bar{t})}{d\cos\theta} = \frac{2\pi\alpha^2 R}{W^2}\beta\frac{\left[2-2\beta^4-\left(1-\xi_2^{(1)}\xi_2^{(2)}\right)(1+\beta^2\cos^2\theta)(1-2\beta^2+\beta^2\cos^2\theta)\right]}{(1-\beta^2\cos^2\theta)^2}. \tag{5.4}$$

Near threshold ($\beta \ll 1$) this expression and its interpretation simplify considerably: for $\xi_2^{(1)} = -\xi_2^{(2)} = \pm 1$, *i.e.*P-wave production, one finds $d\sigma/d\cos\theta \sim \sin^2\theta$ (the forward t, $\bar{t}$ production is forbidden because of momentum conservation); for $\xi_2^{(1)} = \xi_2^{(2)} = \pm 1$ on the other hand, *i.e.*the S-wave case, one obtains a practically isotropic angular distribution.

The answer to the question whether S-wave and P-wave production can be separated experimentally depends on two factors, namely on the relative size of the two cross sections and on the degree of polarization that can actually be achieved.

As can be seen from figs. 1–3 the P-wave cross section is at most a factor of 10–20 smaller than the S-wave production (with the exception of the lowest resonance peak for $m_t = 100$ GeV). Therefore the degree of the photon polarization, $\xi_2^{(1,2)}$ has to exceed 95% to suppress the S-wave contribution below that for the P-wave case. Assuming that electron beams with 90% polarization will become available one expects that high energy photon beams can be prepared with $\sim 97\%$. *This would indeed provide more than adequate suppression of the dominant S-wave production*! The subsequent discussion on the energy distribution of the photon beams will show, as a by-product, that the anticipated S-wave and P-wave excitation curves will actually be more comparable in size thus facilitating their separate measurements.

In the previous sections we have described top production in the collisions of $\gamma\gamma$ beams with a *fixed* energy. This is of course a vast oversimplification of a rather multilayered situation: the photon beams will exhibit a certain energy distribution. The real question then is how wide or how narrow the effective luminosity curve is in energy. There are two concerns one has in this context: Firstly, if the luminosity distribution is too wide, then the threshold enhancement gets very much diluted thus decreasing the sensitivity of the observable excitation curve to m_t and α_S. Secondly, in that case the production cross section would be involved at intermediate energies that are beyond the threshold region proper, yet still not high enough for the Born result to provide a satisfactory approximation; that is where relativistic corrections due to finite width effects etc. come into play; those have not been included in our result. It is clearly quite premature to attempt giving a final answer here concerning the width of the luminosity distributions. Yet the present thinking suggests that

(i) polarized photon beams will actually be more monochromatic than unpolarized photon beams if the circular polarization of the laser beam is set opposite to the longitudinal polarization of the electron beam [5,6]. Technically one would proceed as follows: to obtain the highest degree of monochromaticity of the high energy photon beam one sets the circular polarization of the two laser beams – $\xi(laser\,1)$, $\xi(laser\,2)$ – opposite to the polarization of the electron and of the positron beams – $Pol(e^-)$, $Pol(e^+)$ – i.e. $\xi(laser\,1)\cdot Pol(e^-) < 0$ and $\xi(laser\,2)\cdot Pol(e^+) < 0$; S-wave $t\bar{t}$ production (with $J_z = 0$) can then be studied if both lasers are tuned to have the same circular polarization: $\xi(laser\,1) = \xi(laser\,2)$; P-wave production is then obtained through flipping both the polarization of the electron beam and the laser beam backscattering from it s.t. $\xi(laser\,1)\cdot\xi(laser\,2) < 0$ holds while $\xi(laser\,1)\cdot Pol(e^-) < 0$ is maintained.

(ii) However even so the luminosity curve will not be extremely narrow; it is expected to possess a full width at half maximum of 10–20 GeV.

Such a luminosity distribution has then to be folded with the relevant $\gamma\gamma$ cross sections. In figs. 4 and 5 we show the resulting excitation curves for S-wave and P-wave production for $m_t = 100$ GeV. We plot the cross sections vs. the energy above threshold of the electrons used to produce the polarized photons, and take into account the appropriate luminosity distribution given in the first paper of ref. [5]. We note that one can achieve a high monochromaticity only at the cost of luminosity. In general the luminosity will go approximately as the square of the energy spread. In these conditions, for the S-wave case there is no sharp rise to a plateau passing through the threshold region, and the loss of luminosity may decrease the cross sections up to more than one order of magnitude, because only a fraction of photons are close to the maximum energy. The curves are rather similar for other values of the top mass. From these figures we can draw the following conclusions:

- The resonance peaks have been averaged out. That had to be expected since they require an energy resolution of better than 1 GeV. The excitation curves have then basically lost their sensitivity to the top decay width and to $|V(tb)|$.
- Nevertheless the very sizeable threshold enhancement has survived this averaging and the sensitivity to α_S.

These curves show the trend of the effects; however their specific details should not be viewed as exhibiting the final answers. For we should however keep two things in mind for a proper perspective:

– It would be rather premature (and for these authors also quite inappropriate) to make definite claims about the energy resolution for photon beams that might be achievable ten years from now.

– If however in the end the energy spread cannot be suppressed below 10 GeV, we have to implement a fully relativistic treatment of S-wave as well as P-wave production to gauge the precision of our numerical results. Some relativistic corrections (like the large momentum contribution proportional to the decay width or a relativistic expression for the quark propagator) remain numerically insignificant. Others however that are due to the "running" of the decay width $\Gamma_t(p^2)$ could be potentially sizeable; unfortunately no consensus has developed yet on this subject; see however [15].

6. Conclusions and Outlook

Backscattering polarized laser light off polarized electron beams appears capable of achieving feats that look like miracles performed by Aladdin's lamp:

• The effective luminosity might well exceed that of direct e^+e^- annihilation. A luminosity of $10^{33} cm^{-2} s^{-1}$ actually appears feasible for such a $\gamma\gamma$ collider.

• A relatively high degree of monochromaticity for the resulting photon beams is expected.

• The photon beams are highly energetic and circularly polarized!

All these properties are essential for the analysis that we have discussed here to become feasible:

– Controlling the polarization of the photon beams allows to separate cleanly S-wave and P-wave production of top quarks.

– The relatively good energy definition of the photon beams lets us extract rather directly the threshold enhancements.

– Comparing the values for m_t and α_S obtained from $\gamma\gamma$ collisions with those from e^+e^- annihilation provides us with a crucial systematic cross check on the accuracy with which we have determined these fundamental parameters.

– At present it seems overly optimistic to hope for an energy definition of 1 GeV or better in $\gamma\gamma$ collisions – or in e^+e^- annihilation for that matter. In that case one will be unable to observe the rather dramatic resonance peaks, as shown in figs. 1 and 2. This is a pity since it is unlikely that Γ_t – and thus $|V(tb)|$ – could be measured in any other way.

– Extracting m_t and α_S from P-wave production presents us with another systematically quite independent determination. As stressed before it probes quite different and novel features of QCD dynamics, as contained in the second space derivatives of the $t\bar{t}$ Green's function as opposed to the average of this Green's function that determines S-wave production.

It has to be understood that we have outlined here a general program rather than presented the final algorithm. In particular as far as P-wave production is concerned we have employed a prescription that attempts to mimic some aspects of the scale dependance of α_S, but clearly does not fully incorporate it. Applying it to the S-wave case where we do know the numerical answers shows that the height of the resonance peaks are overestimated by a factor of up to two. However we expect much smaller errors in P-wave production since the resonance peaks are much less prominent there as shown above. The "plateau" heights in the S-wave case between and above the peaks on the other hand show a much smaller sensitivity to the scale dependance of α_S; we expect this feature to hold for P-wave production as well. Nevertheless it would be highly desirable to obtain an algorithm that implements the "running" of α_S in P-wave production [16]. We believe that our discussion gives ample motivation for undertaking such an arduous task.

Acknowledgements

This work was supported in part by National Science Foundation Grant PHY-89-09929, by Department of Energy Contract DE–AC03–76SF00515, and by the United Kingdom Science and Engineering Research Council.

V.A.K. thanks the Theory Group of the Stanford Linear Accelerator Center for the warm hospitality extended to him while this work was being completed.

We have benefitted greatly from illuminating discussions with V.I. Telnov, D. Borden and D. Burke.

After this work was completed we received a paper by Kühn, Mirkes and Steegborn [17], which helped us to correct a small mistake in the expressions for the hard gluon corrections.

References

1. I.I. Bigi *et al.*, Phys. Lett. B 181 (1986) 157.
2. V.S. Fadin and V.A. Khoze, Pis'ma Zh. Eksp. Teor. Fiz. 46 (1987) 417 [JETP Lett. 46 (1987) 525]; Yad. Fiz. 48 (1988) 487 [Sov. J. Nucl. Phys. 48 (1988) 309].
3. V.S. Fadin and V.A. Khoze, Yad. Fiz. 53 (1991) 1118 [Sov. J. Nucl. Phys. 53 (1991) 692];
   I.I. Bigi, V.S. Fadin and V.A. Khoze, Nucl. Phys. B 377 (1992) 461.
4. V.S. Fadin, V.A. Khoze and T. Sjöstrand, Z. Phys. C 48 (1990) 613.
5. D.L. Borden, D.A. Bauer and D.O. Caldwell, preprint SLAC-PUB-5715, UCSB-HEP-92-01 (January 1992), submitted to Phys. Rev. D;
   I.F. Ginzburg *et al.*, Nucl. Inst. Meth. 205 (1983) 47;
   I.F. Ginzburg *et al.*, Nucl. Inst. Meth. 219 (1984) 5.
6. V.P. Gavrilov, I.A. Nagorskaya and V.A. Khoze, Izvestia AN Armenian SSR, Fizika 4 (1969) 137.
7. A.D. Sakharov, Zh. Eksp. Teor. Fiz. 18 (1948) 631;
   A. Sommerfeld, *Atombau und Spektrallinien* (Vieweg, Braunschweig, 1939), Vol. 2.
8. M.J. Strassler and M.E. Peskin, Phys. Rev. D 43 (1991) 1500.
9. J. Schwinger, *Particles, Sources and Fields*, (Addison–Wesley 1973).
10. I. Harris and L.M. Brown, Phys. Rev. 105 (1957) 1656;
    R. Barbieri *et al.*, Nucl. Phys. B 154 (1979) 535.
11. I.I. Bigi and F. Gabbiani, preprint UND-HEP-91-BIG05 (September 1991).
12. R. Barbieri *et al.*, Nucl. Phys. B 192 (1981) 61;
    J.H. Kühn and P.M. Zerwas, Phys. Rep. 167 (1988) 321.
13. K.A. Ispiryan, I.A. Nagorskaya, A.G. Oganesian and V.A. Khoze, Yad. Fiz. 11 (1970) 1278 [Sov. J. Nucl. Phys. 11 (1970) 712].
14. A.I. Akhiezer and V.B. Berestetskii, *Quantum Electrodynamics*, (Interscience Publishers, 1965).
15. Y. Sumino *et al.*, preprint KEK-TH-284 (March 1992);
    H. Muruyama and Y. Sumino, preprint TU-401 (May 1992).
16. M. Jezabek has informed us that he and J.H. Kühn are working on this problem.
17. J.H. Kühn, E. Mirkes and J. Steegborn, preprint TTP92-28 (September 1992).

Figure Captions

Fig. 1 – The cross-section ratio $R_{tt} = \sigma_S(\gamma\gamma \to t\bar{t})/\sigma(e^+e^- \to \mu^+\mu^-)$ for S-wave production and Standard Model top decay is plotted against E in GeV for m_t = 100, 130, 150 and 200 GeV. The solid lines show the full result; the dashed lines show the Born approximation.

Fig. 2 – Same as in Fig. 1, however with a top decay width that is assumed to be 50% larger than the SM width.

Fig. 3 – Same as in Fig. 1, but for P-wave production.

Fig. 4 – The cross-section ratio $R_{tt} = \sigma_S(\gamma\gamma \to t\bar{t})/\sigma(e^+e^- \to \mu^+\mu^-)$ for S-wave production is plotted against the energy above threshold of the electrons E_e in GeV for m_t = 100 GeV after smearing the incoming photon energy by 16 GeV. The solid line shows the full result; the dashed line shows the Born approximation. We assumed a laser photon beam energy of 3.00 eV.

Fig. 5 – The same as in Fig. 4, but for P-wave production.

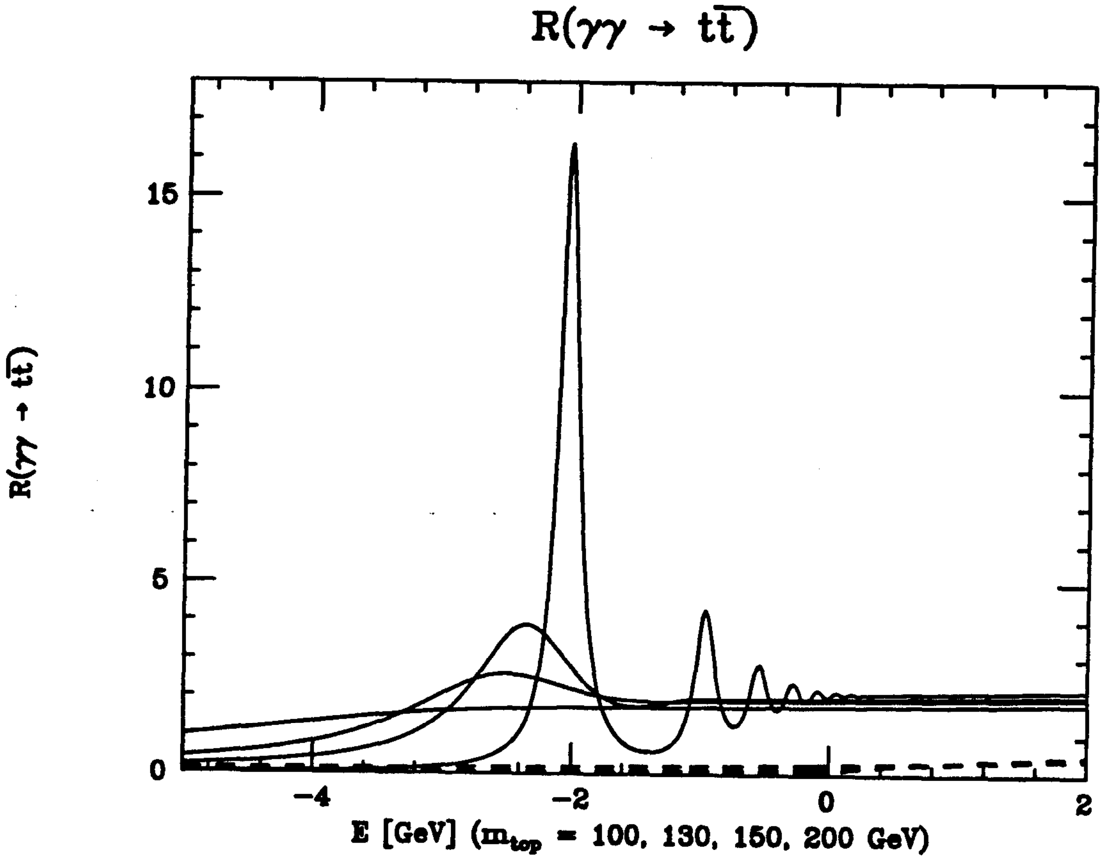

Fig. 1

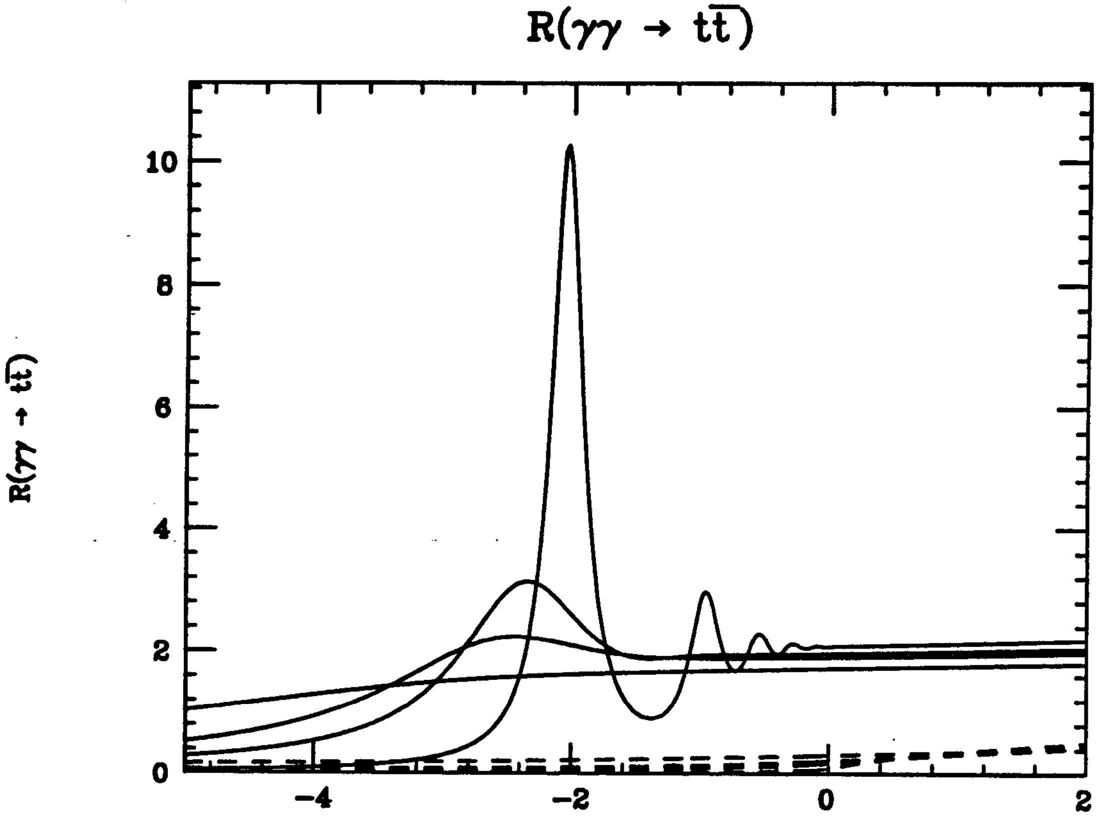

E [GeV] (m_{top} = 100, 130, 150, 200 GeV)

Fig. 2

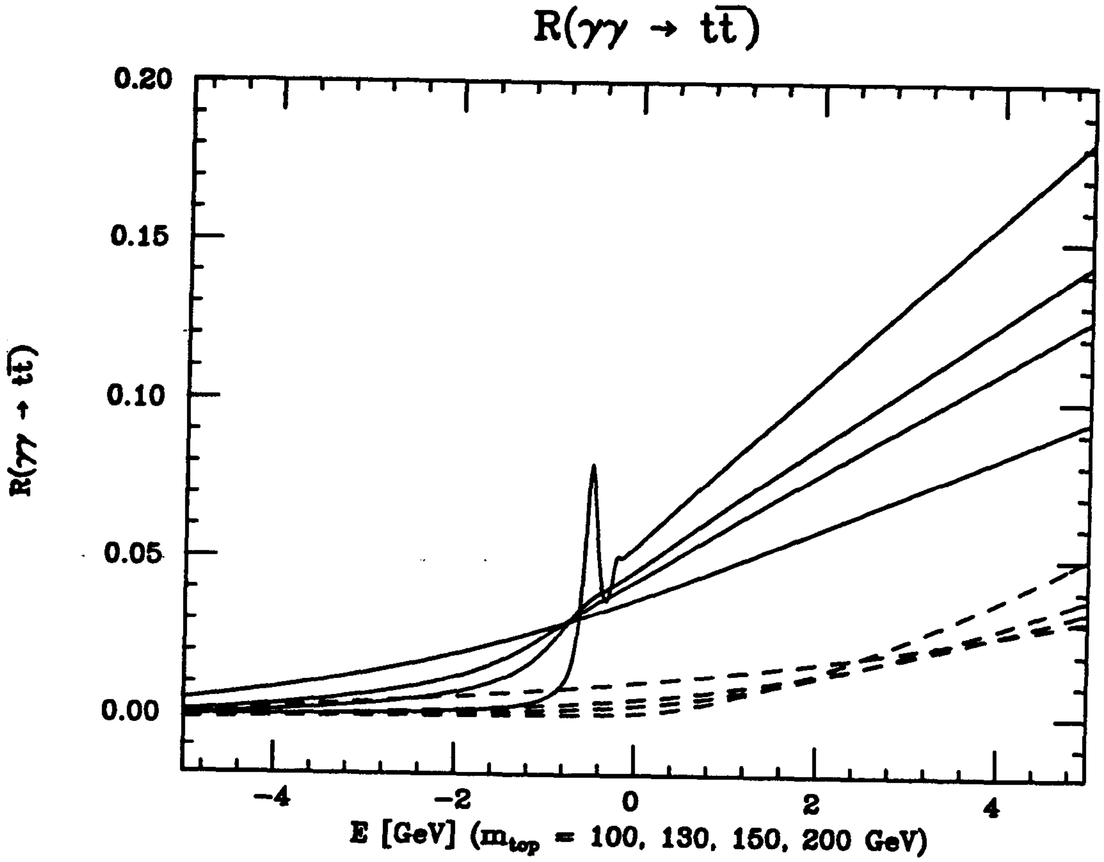
R(γγ → tt̄)
0.20
0.15
0.10
0.05
0.00
R(γγ → tt̄)
−4
−2
0
2
4
E [GeV] (m_top = 100, 130, 150, 200 GeV)
Fig. 3

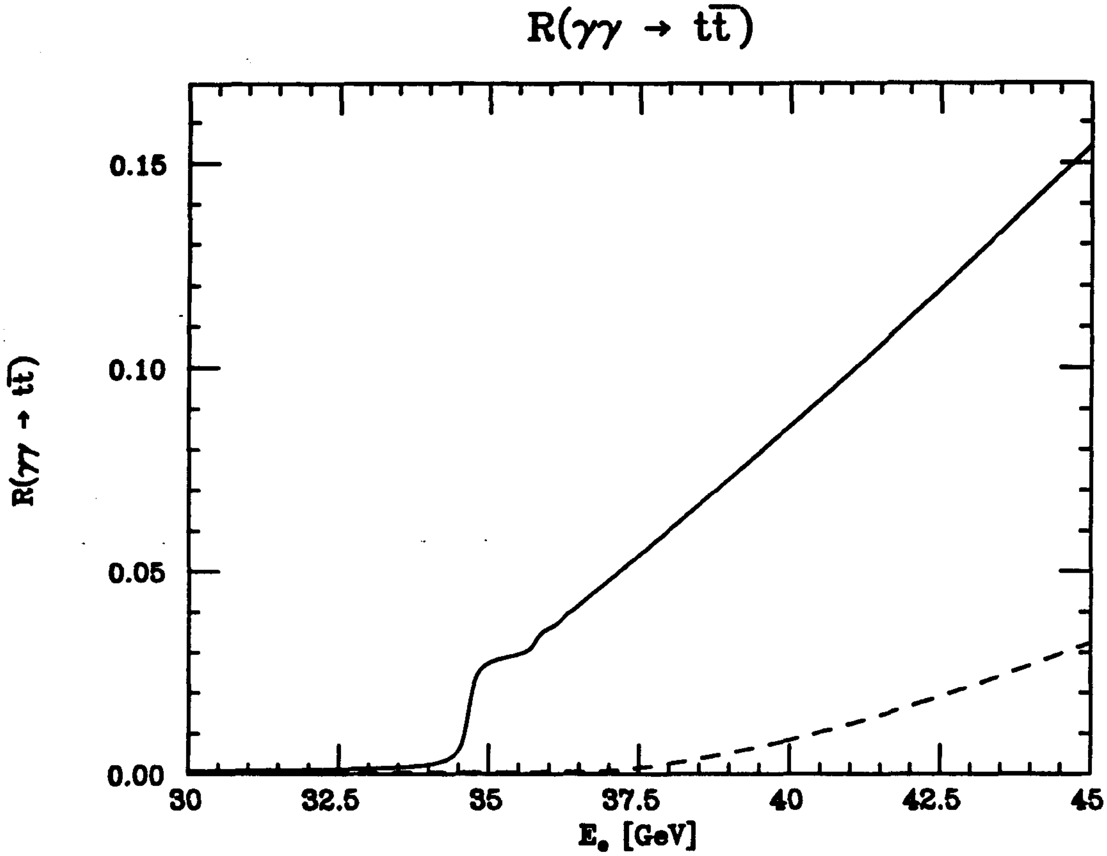

m_{top} = 100 GeV

Fig. 4

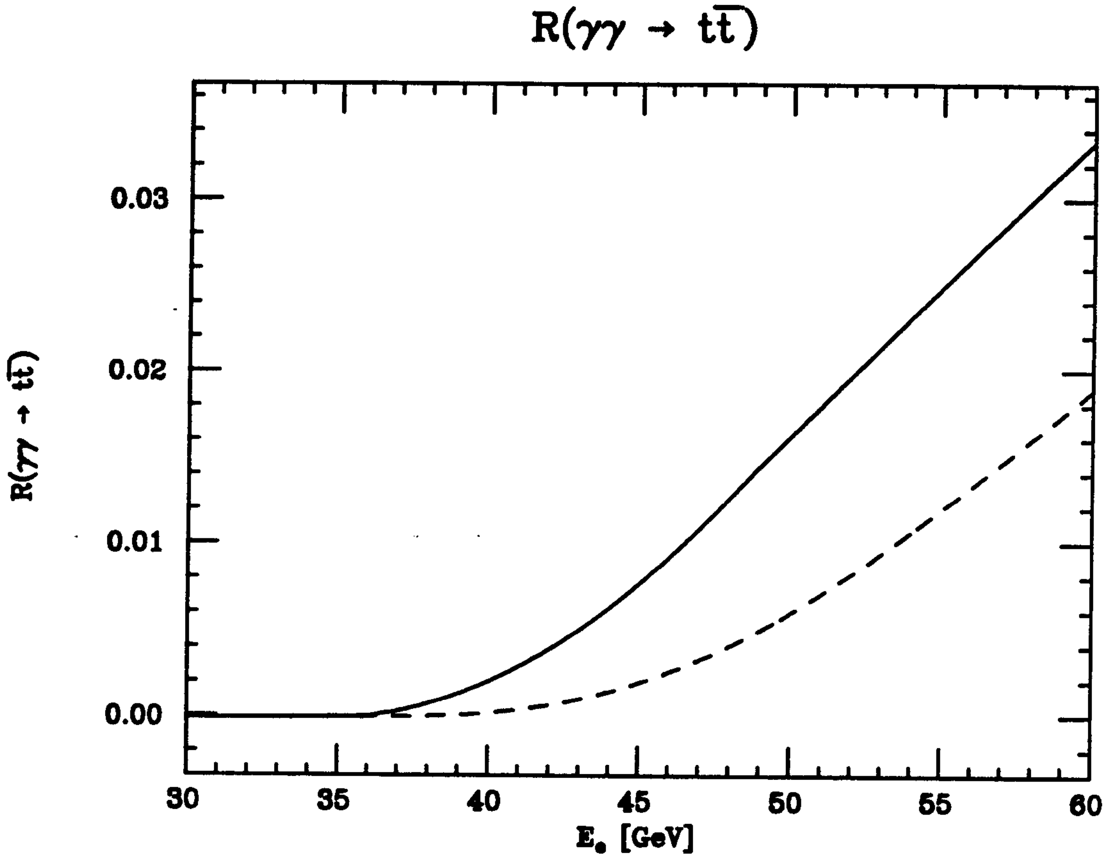

m_{top} = 100 GeV

Fig. 5